Intrinsic defects in $KMgF_3$: the *ab initio* and the extended-ion study

2003 J. Phys.: Condens. Matter 15 4567

(http://iopscience.iop.org/0953-8984/15/26/306)

INSTITUTE OF PHYSICS PUBLISHING JOURNAL OF PHYSICS: CONDENSED MATTER

J. Phys.: Condens. Matter **15** (2003) 4567–4576 PII: S0953-8984(03)59831-9

Intrinsic defects in $KMgF_3$: the *ab initio* and the extended-ion study

G Q Huang[1,2,4], L F Chen[2], Mei Liu[3] and D Y Xing[1]

[1] National Laboratory of Solid State Microstructures, Department of Physics, Nanjing University, Nanjing 210093, China
[2] Department of Physics, Nanjing Normal University, Nanjing 210097, China
[3] Department of Physics, Southeast University, Nanjing 210096, China

E-mail: ghuang@email.njnu.edu.cn

Received 20 February 2003
Published 20 June 2003
Online at stacks.iop.org/JPhysCM/15/4567

Abstract

The intrinsic defects in $KMgF_3$, such as V_K centres and self-trapped excitons (STEs), are studied by the *ab initio* method and the extended-ion method. In the *ab initio* method, the Madelung potentials are introduced into the Fock operator terms to perform calculations on clusters modelling ionic solids. It is found that the V_K centre moves toward the nearby interstitial site, still keeping C_{2v} symmetry; and the STE is unstable in the on-centre symmetry, undergoing a relaxation consisting of an axial translation superimposed with a rotation. Such a translation plus rotation relaxation of the STE in $KMgF_3$ is quite different from those in alkali halides and in alkali-earth halides. The calculated results for the excitation energy of the V_K centre and for the emission energy of the STE are in reasonable agreement with experiments.

1. Introduction

$KMgF_3$ single crystals are known to have wide application as fast UV scintillators [1]. Suitably doped crystals have been successfully used in tunable solid state lasers [2] and in radiation dosimetry [3]. Even though the properties of rare-earth element doped $KMgF_3$ have been extensively investigated from practical viewpoints [4, 5], little is known about intrinsic defects in the host. In order to understand optoelectronic processes in the host, the knowledge of the intrinsic defects is indispensable.

The details of hole motion in the ion crystal are well understood. At low temperatures, if the electron is ionized from one of the halide ions and is trapped elsewhere, the self-trapped hole, which is called the V_K centre, will be formed. It is a hole trapped between two adjacent anions and can be looked on as a molecular ion X_2^- embedded in the host crystal. When an electron

[4] Author to whom any correspondence should be addressed.

0953-8984/03/264567+10$30.00

is captured by a self-trapped hole, it may form a self-trapped exciton (STE). The relaxation of the STE leads to the formation of the F–H centre pair. The F centre is a typical colour centre consisting of an electron trapped at an anion vacancy. The H centre is an interstitial halogen atom bonded covalently to the site anion. It is a homonuclear diatomic defect with asymmetric hole distribution. Experimentally, the V_K absorption band has its peak at 3.7 eV with width of 0.9 eV [6]. Thermal reorientation of the V_K centre occurs by $\pi/2$ jumps of the molecular axis of the hole trap centre with an activation energy of 0.26 eV and by $\pi/3$ jumps with an activation energy of 0.29 eV [7]. Alcala *et al* [8] identified the intrinsic luminescence of $KMgF_3$ as being of STE origin. The STE luminescence band is about 3.65 eV. The optically detected magnetic resonance of STE in $KMgF_3$ was studied by Hayes *et al* [9], confirming that the STE luminescence is emitted from a triplet state.

Various calculations [10–12] of the STEs in alkali halides (AHs) have been presented both by the extended-ion method and by the *ab initio* method. The off-centre structure of the STEs in AHs, which was predicted by Song and co-workers [10–12], has been established. Recently, Gavartin *et al* [13] attempted to model charge self-trapping in NaCl within the density functional theory. Furthermore, quantum chemical INDO calculations were used to model the polarons and excitons in ABO_3 perovskite crystals [14–17]. But, to the best of our knowledge, there has been no corresponding theoretical study in perovskite-structural halides. The objective of this paper is to study theoretically the structure of the V_K centre and STE in $KMgF_3$. Two computational methods, the extended-ion method [12] and the *ab initio* method based on the modified GAUSSIAN 94 (G94) [18], are used. In the *ab initio* method, the Madelung potentials have been included in the Fock operator terms to perform calculations on clusters modelling ionic solids. Both methods reveal that the V_K centre moves toward the nearby interstitial site, keeping the molecular axis still along the [110] direction, but the rotation of the H centre is necessary for the formation of a stable STE. The structure of the STE and its decay behaviour are studied and compared with those in other ionic crystals. The calculated results for the excitation energy of the V_K centre and the emission energy of the STE are in good agreement with experiment.

2. Methods of calculation

The *ab initio* calculation is based on the G94 code. The quantum cluster is partitioned into two regions. The inner region I includes the defect, its nearest and sometimes the next-nearest neighbours. The defect is at the centre of region I, all ions in which are allowed to move. The outer region II includes all the nearest and the next-nearest neighbours of the surface ions of region I. It can prevent the surface ions of the region I from undergoing unphysical displacements in the course of geometry optimization. The G94 code has been modified to create the infinite ionic crystal field effect by the Ewald method [19]. The calculated Madelung potential enters the Fock matrix and the Hartree–Fock–Roothaan equation is then solved self-consistently.

The Hartree–Fock energy of an isolated cluster can be expressed as

$$E^0 = \sum_{\mu\nu} P_{\mu\nu} h_{\mu\nu} + \tfrac{1}{2} \sum_{\mu\nu\lambda\sigma} P_{\mu\nu\lambda\sigma} (\mu\nu|\lambda\sigma) + V_{nuc} \tag{1}$$

where $P_{\mu\nu}$ and $P_{\mu\nu\lambda\sigma}$ are the one- and two-particle density matrices, respectively. $h_{\mu\nu}$ and $(\mu\nu|\lambda\sigma)$ are the one- and two-electron integrations, respectively. V_{nuc} is the nuclear–nuclear repulsive energy. When the cluster is embedded in the ionic crystal, the Hartree–Fock energy

is given by

$$E' = E^0 + \sum_{\mu\nu} P_{\mu\nu}\langle\chi_\mu(\boldsymbol{r}-\boldsymbol{R}_A)|\sum_{j=N+1}^{+\infty}\frac{Q_j}{|\boldsymbol{r}-\boldsymbol{R}_j|}|\chi_\nu(\boldsymbol{r}-\boldsymbol{R}_B)\rangle + \sum_{i=1}^{N} Z_i(A)\sum_{j=N+1}^{+\infty}\frac{Q_j}{|\boldsymbol{R}_A-\boldsymbol{R}_j|}. \tag{2}$$

The second and third terms are the interaction energies for the electrons and the nuclei of the cluster, respectively, with the remaining ionic crystal. Here, N is the number of cluster ions, Z is the nucleus charge of the ion in the cluster and Q_j is the net charge of the remaining ion with $Q_{F^-} = -1(e)$, $Q_{K^+} = +1(e)$, and $Q_{Mg^{2+}} = +2(e)$. We define $\varphi_i{}'(A)$ as

$$\varphi_i{}'(A) = \sum_{j=N+1}^{+\infty}\frac{Q_j}{|\boldsymbol{R}_A-\boldsymbol{R}_j|}, \tag{3}$$

which is the cluster-subtracted Madelung potential at the quantum nucleus site A. The Madelung potentials are evaluated using the Ewald method [19]. The cluster-subtracted Madelung potentials are obtained by subtracting from the Madelung potentials those contributions arising from the other ions comprising the quantum cluster. We take $\varphi' = \varphi'(A)$ for the diagonal matrix element with $\mu, \nu \in A$; and $\varphi' = \frac{1}{2}[\varphi'(A)+\varphi'(B)]$ for the off-diagonal matrix element with $\mu \in A$, $\nu \in B$. Equation (2) may be approximated as

$$E' \simeq E^0 + \sum_{\mu\nu} P_{\mu\nu}\varphi'\langle\chi_\mu(\boldsymbol{r}-\boldsymbol{R}_A)|\chi_\nu(\boldsymbol{r}-\boldsymbol{R}_B)\rangle + \sum_{i=1}^{N} Z_i(A)\varphi_i'(A). \tag{4}$$

This approximation is very similar to that used in [20], in which it was justified to be reliable beyond the range of so-called Madelung radii (several ånstroms). In this paper, since the ions in region I which are allowed to move are surrounded by the outer region II, this approximation is reasonable for the ions in region I and is unlikely to affect our results. In our embedded cluster method, the quantum cluster is embedded into the infinite ionic crystals; the problem of the poor convergence about the long-range Coulomb potential is handled by introducing the Ewald method. This embedded method is different from that in [21] and [22], in which a quantum cluster is embedded into a large finite polarizable lattice represented by the shell model.

An important consideration for the *ab initio* calculation is the choice of basis sets. Although neutral atom basis sets are compiled by Huzinaga [23], we sometimes find they are not suitable for studying the defects in ionic crystals from the analysis of the Mulliken population. The wavefunctions of K^+, Mg^{2+} and F^- within region I are taken from the Slater-type Hartree–Fock expansion functions of ions [24] and then fitted to eight Gauss-type orbital (GTOs). The wavefunction of the fluorine ion forming a V_K centre or an H centre is taken as an average of the Slater-type Hartree–Fock expansion functions of F^0 and F^- and then fitted to eight GTOs. To test this chosen basis we have calculated the equilibrium bond length and optical transition energies ($\Sigma_u \Rightarrow \Sigma_g$ and $\Sigma_u \Rightarrow \pi_g$) for an isolated molecular ion F_2^-. The calculated results are found in reasonable agreement with those calculated in the molecular-orbital self-consistent-field approximation [25]. In region II, F^- are also represented by the fitted eight GTOs, whereas K^+, Mg^{2+} are replaced respectively by LANL1 and CHF pseudo-potentials [18] (no basis used) in order to reduce the computational time. For an exciton, a ghost atom [18] with the optimized basis functions is used to model the excited electron. The triplet exciton state can be handled by an unrestricted Hartree–Fock (UHF) calculation, in which the number of bases used is the same as the number of occupied 'alpha electron' orbitals.

G94 is based on the quantum chemical theory; it is more accurate especially in calculating the optical absorption or luminescence energy of the defect system. However, its computation time is in great demand and it is not suitable for studying the diffusion of a V_K centre or H centre where a big cluster has to be adopted. As a result, the extended-ion method is used in this study. It is found that numerical results obtained by the two methods are close to each other.

In the extended-ion method, the excited electron is studied by the hybrid method within the framework of the one-electron Hartree–Fock approximation. The defect electron wavefunction ψ is required to be orthogonal to the occupied orbitals of the crystal ion, yielding

$$|\psi\rangle = |\varphi\rangle - \sum_{\nu l} |\chi_{\nu l}\rangle\langle\chi_{\nu l}|\varphi\rangle, \tag{5}$$

where $\chi_{\nu l}$ is the occupied orbital ν at site l, and φ is represented by a linear combination of floating 1s Gaussians. The secular determinant is solved for this wavefunction. The occupied ionic orbitals χ are divided into two groups. The terms from the deeper electron shells in the secular determinant are represented by the 'ion-size' parameters. For the outermost s and p shells, all the required terms (the screened Coulomb term, exchange term and overlap term) in the secular determinant are calculated explicitly and suitable interpolation formulae are devised. For an exciton, there are two open shells in the electron configuration. Only the exchange interaction between the electrons on the molecular ion with an open shell and the excited electron depends on the spin state. For the spin triplet state, the exchange integral is the same as that for a closed shell. A detailed description of this hybrid method was given in [12]. The long-range Coulomb energy is treated by the Ewald summation [19]. The interactions between ions as well as the polarization are classically treated, respectively, using the Born–Mayer type pair potentials and polarizable dipole approximation. The molecular ions sharing the hole are represented by a CNDO code. The hole charge distribution resulted from the CNDO calculation is imported into the extended-ion package as it is needed. At the same time, the CNDO energy depends on the electrostatic potential produced by the lattice ions as well as the defect electron. The two parts iterate constantly to maintain consistency during the lattice relaxation. In determining the equilibrium structure of the defect system, the minimization routine of its total energy is improved by relaxing all ions at the same time [26]. This approach leads to an improved symmetry of the ionic displacement around the defect.

3. Results and discussions

$KMgF_3$ has the perovskite structure, in which a K^+ ion resides at the centre of a cubic unit cell with Mg^{2+} at each corner; the F^- ions are centred on each crest line, as shown in figure 1. The lattice constant is $a_0 = 7.51$ au. The V_K centre is a hole trapped between two adjacent anions oriented along the [110] direction as illustrated by the dashed lines in figure 1 and can be looked on as a molecular ion F_2^- embedded in the host crystal. We first optimize the structure of the V_K centre in $KMgF_3$ by the extended-ion method. The V_K centre and its nearest and next-nearest neighbour ions (total 23 ions as labelled in figure 1) are allowed to move. The calculated results of the distorted displacements are tabulated in table 1, in which only those ions with distortion larger than 2% of a_0 are included. It is found that the most important relaxation is between the two ions forming the V_K centre. The distance between them is obtained as about 3.54 au, much smaller than 5.31 au, the value in a perfect crystal. It follows that the covalent bonded F_2^- molecular ion has formed. From the structure of the V_K centre shown in figure 1, we can see that the V_K centre moves toward the nearby interstitial site (I.S. shown in figure 1), but keeping the molecular axis still along the [110] direction. The symmetry of the V_K centre is C_{2v}, while it is D_{2h} in AHs. This difference is caused by the different crystal structures.

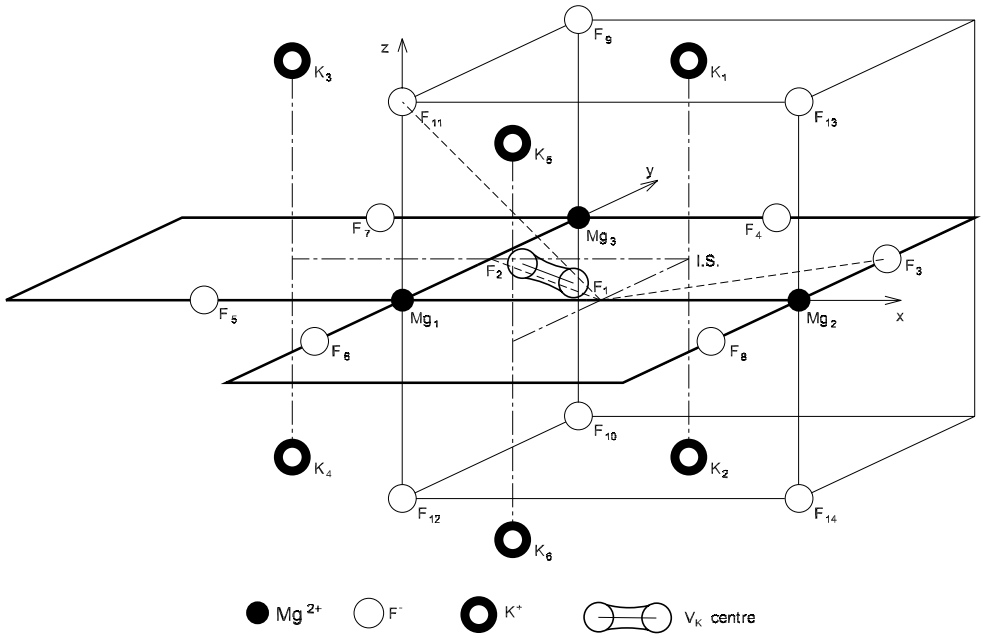

Figure 1. The cluster of ions which are allowed to move in the study of the V_K centre. The optimized geometrical structure of the V_K centre is sketched.

We also study the V_K centre by the *ab initio* code. The quantum cluster used consists of 23 ions in region I as shown in figure 1 and 65 ions in region II. We first test the quality of the basis functions employed and the embedding procedure by examining the stability of the chosen quantum cluster. A full geometry optimization of the ground-state perfect cluster is performed. The largest ion displacements in region I are about 0.04 Å. This indicates that our approach is reliable and reasonable. We then optimize the geometry structure of the defect cluster including the V_K centre. The results of distorted configurations in region I are given by the values within the brackets in table 1. It is found that the calculated results obtained from the two methods are close to each other. For example, the bond length of the F_2^- obtained from the *ab initio* calculation is 3.62 au, slightly larger than 3.54 au from the extended-ion method.

In order to study the reorientation of the V_K centre, we need to use a bigger cluster. In this calculation only the extended-ion method is used, for it is difficult to use the *ab initio* method when the cluster is fairly big. For the study of the $\pi/2$ jump, three F^- ions (F_1, F_2 and F_3 shown in figure 1) are treated by the CNDO code. At the beginning, the covalent bond is assumed to be along the [110] direction, indicating a covalent bond between ion F_1 and F_2. Then let F_1 move toward F_3 in several steps and minimize the total energy at each step by allowing the surrounding ions to relax. Finally, it is found that a covalent bond between F_1 and F_3 is formed; at the same time, F_2 moves to its corresponding position in a perfect crystal. This is a bond-switching from the [110] to the $[1\bar{1}0]$ direction. For the $\pi/3$ jump of the V_K centre, we have performed a similar simulation, three F^- ions (F_1, F_2 and F_{11}) treated by the CNDO code. The molecule bond is transformed from the [110] to the [101] direction. The calculated energy barriers in the processes of bond-switching are about 0.33 and 0.38 eV, respectively, for the $\pi/2$ and the $\pi/3$ jump. They are close to but slightly larger than the experimental values of the activation energy [7] (0.26 and 0.29 eV, respectively).

For the STE study, two FGOs are positioned on the [110] axis at the perfect lattice sites occupied by the molecular ions. The optimized FGO exponent is 0.08 au. The geometry

Table 1. The distorted displacements along the x, y, and z directions (Δx, Δy, and Δz) around the V_K centre and the STE. The first values and those within the brackets are obtained from the extended-ion calculations and the *ab initio* calculations, respectively. F_1 and F_2 stand for two ions that form the V_K centre or H centre. The second column indicates the coordinates of the ions in a perfect crystal. The displacements and the coordinates are in units of the lattice constant a_0. Only ions with displacement larger than 2% of a_0 are listed.

	Ion	Ion Coordinates	Δx	Δy	Δz
	F_1	(0.5, 0.0, 0.0)	−0.05(−0.05)	0.12(0.11)	0.00(0.00)
	F_2	(0.0, 0.5, 0.0)	0.12(0.11)	−0.05(−0.05)	0.00(0.00)
	Mg_1	(0.0, 0.0, 0.0)	−0.05(−0.04)	−0.05(−0.04)	−0.00(−0.00)
	Mg_2	(1.0, 0.0, 0.0)	0.03(0.03)	0.00(0.01)	−0.00(−0.00)
	Mg_3	(0.0, 1.0, 0.0)	0.00(0.01)	0.03(0.03)	−0.00(−0.00)
V_K	K_1	(0.5, 0.5, 0.5)	0.02(0.02)	0.02(0.02)	0.05(0.04)
	K_2	(0.5, 0.5, −0.5)	0.02(0.02)	0.02(0.02)	−0.05(−0.04)
	F_5	(−0.5, 0.0, 0.0)	0.00(−0.00)	0.03(0.05)	0.00(0.00)
	F_6	(0.0,−0.5, 0.0)	0.03(0.05)	0.00(−0.00)	0.00(0.00)
	F_7	(−0.5, 1.0, 0.0)	0.02(0.03)	−0.03(−0.07)	0.00(0.00)
	F_8	(1.0, −0.5, 0.0)	−0.03(−0.07)	0.02(0.03)	0.00(0.00)
	F_1	(0.5, 0.0, 0.0)	0.05(0.03)	−0.07(−0.09)	0.01(0.01)
	F_2	(0.0, 0.5, 0.0)	0.37(0.41)	−0.14(−0.14)	0.00(0.00)
	Mg_1	(0.0, 0.0, 0.0)	−0.07(−0.02)	0.05(−0.02)	−0.01(−0.01)
	Mg_2	(1.0, 0.0, 0.0)	0.05(0.03)	−0.00(0.00)	−0.01(−0.00)
	Mg_3	(0.0, 1.0, 0.0)	0.01(0.00)	−0.06(0.03)	−0.00(−0.00)
	K_1	(0.5, 0.5, 0.5)	0.01(0.03)	0.03(0.02)	0.08(0.07)
STE	K_2	(0.5, 0.5, −0.5)	0.01(0.03)	0.03(0.02)	−0.07(−0.07)
	K_3	(−0.5, 0.5, 0.5)	−0.01(−0.01)	0.01(−0.01)	0.02(0.04)
	K_4	(−0.5, 0.5, −0.5)	−0.01(−0.01)	0.02(−0.01)	−0.02(−0.04)
	F_4	(0.5, 1.0, 0.0)	0.01(−0.00)	0.04(0.02)	0.00(0.00)
	F_5	(−0.5, 0.0, 0.0)	0.00(−0.01)	−0.03(−0.02)	0.00(0.00)
	F_6	(0.0, −0.5, 0.0)	0.02(−0.01)	−0.03(−0.01)	0.00(0.00)
	F_9	(0.0, 1.0, 0.5)	0.00(0.00)	0.02(0.03)	0.01(0.00)
	F_{10}	(0.0, 1.0, −0.5)	0.01(0.00)	0.02(0.03)	−0.01(−0.00)

optimizations of this defect system are performed by the extended-ion method and the *ab initio* method. The adopted quantum cluster is the same as that in the V_K study. The stable geometrical structure of the STE is illustrated in figure 2. With the molecular ions displacing from the on-centre geometry, the electron is immediately localized on one vacancy site. So only one FGO is illustrated in figure 2. The molecular axis is not along the original [110] direction. The molecular ion shifts along [110] and meanwhile rotates toward [010] where the interstitial site is located. The angles of the rotation are about 22° and 29°, respectively, by the extended-ion calculation and the *ab initio* method. The calculated results for the distorted displacements of those ions which are larger than 2% of a_0 are also tabulated in table 1. The ions around the excited electron represented by 'FGO' have large displacements. The two methods give the similar distortions for the molecular ions, but have some differences for other ions. For example, the Mg_3 ion even has different displacement direction. This may stem from the fact that the short-range interactions between the defect electron and the ions are not well reproduced in the extended-ion method.

In order to study the possibility of a larger separation between the electron and hole, the adiabatic-potential-energy surfaces (APESs) are calculated by the extended-ion method. Three F^- ions (F_1, F_2 and F_8 in figure 2) are treated by the CNDO code. In the initial configuration,

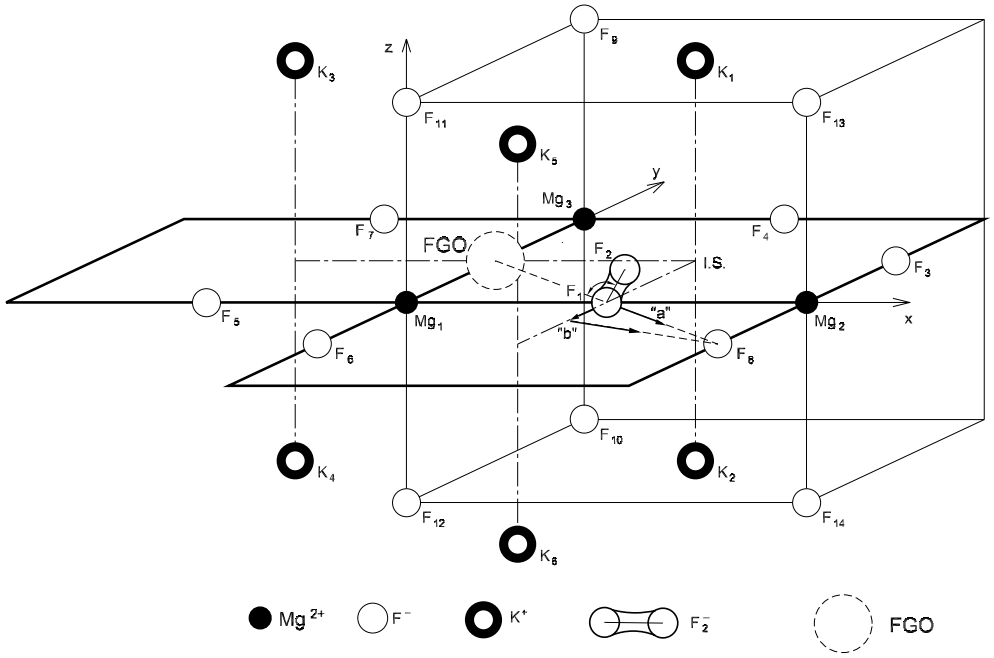

Figure 2. The cluster of ions which are allowed to move in the study of the STE. The optimized geometrical structure of the STE and the two possible pathways 'a' and 'b' of the STE decay are sketched.

the covalent bond is formed between F_1 and F_2 as shown in figure 2. Then let F_1 move toward F_8 in several steps and minimize the total energy at each step by allowing the surrounding ions to relax. Two possible pathways for the F_1 movement are chosen, as illustrated by 'a' and 'b' in figure 2. For path 'a', F_1 moves 2.5 au in five steps along the [110] row of fluorides. For path 'b', F_1 first moves 1.5 au in three steps along the [010] direction and then moves 1.5 au in three steps toward the F_8. It is found that the molecule bond is formed between F_1 and F_8 in the final step for both paths 'a' and 'b'. However, the molecular bonds have different orientations for the two cases. The calculated APESs as a function of the distance d between the F centre and H centres are shown in figure 3. The position of the H centre is defined as the position of the centre of gravity of the hole charge distributed on the three fluorine ions (F_1, F_2 and F_8). The energies are plotted with respect to that of the perfect lattice. The APES for path 'b' is relatively flat, while for path 'a' the energy rises monotonically on the trajectory of further F–H separation. Since the energy for path 'b' is always lower than that for path 'a', the separation between the electron and hole is favourable for path 'b'. This may be associated with the asymmetry on both sides of the [110] row of fluorides.

We wish to point out that the geometrical structure of the STE in $KMgF_3$ is of a new type of configuration, quite different from those in AHs and in alkali-earth halides (AEHs). In all three kinds of ionic crystal (AHs, AEHs and $KMgF_3$), the STE is unstable for the on-centre symmetry. However, the different crystal structures result in different configurations of the STE in them. First, the relaxation of the STE in AHs is an axial translation along the [110] row of halides. Previous studies [10–12] confirm that the STE in AHs undergoes a symmetry-breaking axial relaxation, leading to a separation of the electron and hole. The amount of axial translation depends significantly on the type of AH. Kan'no *et al* [27] observed the π-band

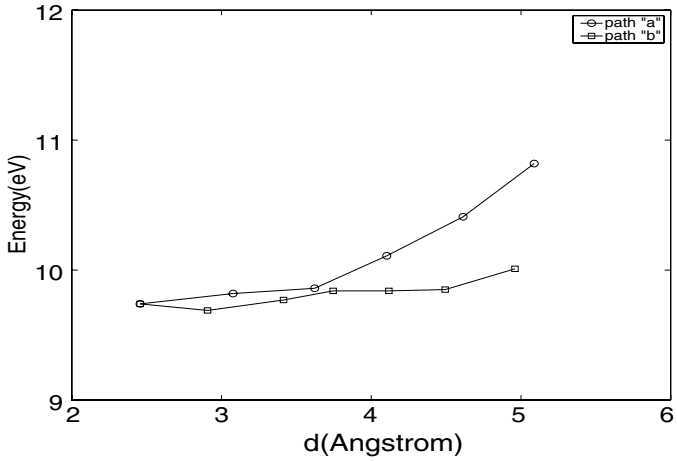

Figure 3. The APESs of the STE for two possible trajectories are plotted as functions of the distance d between F and H centres. The position of the H centre is defined as the position of the centre of gravity of the hole charge. Path 'a' and path 'b' are defined in the text and sketched in figure 2.

Stokes shift to the free exciton absorption energy and concluded that there are three types of STE in AHs. Calculations by Song *et al* [10, 12] showed that the type I STE should probably be described as 'nearly on centre'. This group is typified by NaBr with a large molecular ion in a small lattice. Type III STE was attributed to the off-centre STE with configuration close to the nearest-neighbour F–H pair. In this group the molecule is relatively small compared with the lattice constant. Type II is then an intermediate degree of off-centre relaxation. Second, the relaxation of the STE in AEHs is a rotation of the molecular ions from the [100] to the [111] direction. According to the studies of optically detected magnetic resonance [28] and the theoretical calculation [29], the STE in AEHs is equivalent to the nearest-neighbour F–H pair with the F_2^- molecular axis along the [111] crystal axis, one of the bonded halide ions on a substitutional site and the other on an interstitial site. Finally, the present calculated result shows that the STE in $KMgF_3$ undergoes a relaxation consisting of an axial translation superimposed with a rotation from the [110] toward the [010] direction, as sketched in figure 2. As a result, it is a new type of STE, whose relaxation is neither a simple translation as in AHs nor a pure rotation as in AEHs. Furthermore, we want to mention that the structure of the STE in the $KMgF_3$ ionic crystal is also different from that in partly covalent ABO_3 perovskites [14–17]. Quantum chemical INDO calculations combined with the periodic defect model have demonstrated that the triplet exciton for example in $BaTiO_3$ is a triad centre consisting of one active O atom (O_1) and two Ti atoms. The main effect is the charge transfer from the O_1 atom onto the nearest Ti_1 atom. These two atoms are displaced toward each other, whereas another Ti_2 atom experiences a repulsion from the O_1 atom and is displaced outwards. So, the exciton in oxide perovskites is also called the charge transfer vibronic exciton.

The polarization pattern of the STE is the same in AHs and $KMgF_3$. The electron is well localized on the halide ion vacancy and the hole is mainly localized on the halide ion nearest to the electron. The hole distribution in $KMgF_3$ by our calculations is 0.26 (F_1) and 0.74 (F_2) with F_2 nearest to the excited electron. However, there are some differences in the conversion from STEs to the Frenkel F–H defect pair between the two kinds of lattice. In AHs all three types of STE can be further separated with energy barrier no larger than about

0.2 eV [11]. The existence of a [110] row of halide ions plays an important role in promoting the efficient bond-switching sequence of the halide molecular anion, leading to a low barrier for F–H pair separation. In $KMgF_3$, although it has a [110] row of fluorides, the decay of the STE is not along the [110] row because of the asymmetry on both sides of the [110] row. Further separation of the STE into a second-neighbour F–H pair may be along path 'b', as discussed above, involving bond-switchings mediated by rotations. Such a difference may originate from the difference in crystal structure between AHs and $KMgF_3$.

The optical absorption and emission energies of the intrinsic defects are calculated by using the UHF method in the G94 code. For the V_K centre, the main optical absorption transition is $\Sigma_u \Rightarrow \Sigma_g$. The calculated transition energy is 3.96 eV, which is in good agreement with the experimental peak energy, 3.7 eV, of the V_K absorption band [8]. The emission energy of the STE is taken as the difference in energy between the stable triplet STE and the ground state with the same ion positions. Our calculated value of the emission energy is 4.06 eV, and the experimental value is about 3.65 eV [6], in reasonable agreement with each other.

In summary, the V_K centre and STE in $KMgF_3$ have been studied by the extended-ion method and the *ab initio* method. Very close calculated results are obtained from the two methods. It seems reasonable and reliable to use the Madelung potentials instead of hundreds and thousands of fixed point charges to perform calculations on clusters modelling ionic solids. The V_K centre moves toward the nearby interstitial site, still keeping C_{2v} symmetry. The STE is unstable in the on-centre symmetry, undergoing a relaxation consisting of an axial translation superimposed with a rotation. The structure of the STE and its decay behaviour are studied and compared with those in other ionic crystals. The calculated result of the excitation energy of the V_K centre and the emission energy of STE by the UHF method in the G94 code are in reasonable agreement with experimental data.

References

[1] Jansons I L, Krumins V J, Rachko Z A and Valbis J A 1988 *Solid State Commun.* **67** 183
[2] Horsch G and Paus H J 1986 *Opt. Commun.* **60** 69
[3] Bacci C, Fioravanti S, Furetta C, Missori M, Ramogida G, Rossetti R, Sanipoli C and Scacco A 1993 *Radiat. Prot. Dosim.* **47** 277
[4] Gektin A V, Komar V K, Shlykhturov V V and Shiran N V 1996 *IEEE Trans. Nucl. Sci.* **43** 1295
[5] Gektin A V 2000 *J. Lumin.* **87–89** 1283
Seo H J, Moon B K and Tsuboi T 2000 *J. Lumin.* **87–89** 1059
[6] Riley C R and Sibley W A 1970 *Phys. Rev.* B **1** 2789
Hall T P P and Leggeat A 1969 *Solid State Commun.* **7** 1657
[7] Lewis J T, Kolopus J L, Sonder E and Abraham M M 1973 *Phys. Rev.* B **7** 810
[8] Alcala R, Koumvakalis N and Sibley W A 1975 *Phys. Status Solidi* a **30** 449
[9] Hayes W, Owen I B and Pilopenko G I 1975 *J. Phys. C: Solid State Phys.* **8** L407
[10] Song K S, Leung C H and Williams R T 1989 *J. Phys.: Condens. Matter* **1** 683
Song K S and Leung C H 1989 *J. Phys.: Condens. Matter* **1** 8425
[11] Shluger A L, Grimes R W and Catlow C R A 1991 *J. Phys.: Condens. Matter* **3** 3125
Song K S and Baetzold R C 1992 *Phys. Rev.* B **46** 1960
Baetzold R C and Song K S 1991 *J. Phys.: Condens. Matter* **3** 2499
[12] Williams R T and Song K S 1993 *Self Trapped Exciton (Springer Series in Solid State Science)* (Berlin: Springer) p 53
[13] Gavartin J L, Sushko P V and Shluger A L 2003 *Phys. Rev.* B **67** 035108
[14] Eglitis R I, Kotomin E A, Borstel G, Kapphan S E and Vikhnin V S 2003 *Comput. Mater. Sci.* **27** 81
[15] Eglitis R I, Kotomin E A, Trepakov V A, Kapphan S E and Borstel G 2002 *J. Phys.: Condens. Matter* **14** L647
[16] Eglitis R I, Kotomin E A and Borstel G 2002 *Eur. Phys. J.* B **27** 483
[17] Eglitis R I, Kotomin E A, Borstel G and Vikhnin V S 2002 *Ferroelectrics* **268** 479
[18] Frisch M J *et al* 1994 *Gaussian 94* (Pittsburgh, PA: Gaussian)
[19] Kittel C 1956 *Introduction to Solid State Physics* (New York: Wiley) p 571

[20] Saalfrank P 1991 *J. Phys.: Condens. Matter* **3** 2621
[21] Sushko P V, Shluger A L, Baetzold R C and Catlow C R A 2000 *J. Phys.: Condens. Matter* **12** 8257
[22] Sushko P V, Shluger A L and Catlow C R A 2000 *Surf. Sci.* **450** 153
[23] Huzinaga S 1984 *Gaussian Basis Sets for Molecular Calculations* (New York: Elsevier)
[24] Clementi E and Roetti C 1974 *At. Data Nucl. Data Tables* **14** 178
[25] Gilbert T L and Wahl A C 1971 *J. Chem. Phys.* **55** 5247
[26] Fu C R, Chen L F and Song K S 1999 *J. Phys.: Condens. Matter* **11** 5699
[27] Kan'no K, Tanaka K and Hayashi T 1990 *Rev. Solid State. Sci.* **4** 383
[28] Call P J, Hayes W and Kabler M N 1975 *J. Phys. C: Solid State Phys.* **6** L60
[29] Adair M, Leung C H and Song K S 1985 *J. Phys. C: Solid State Phys.* **18** L909